2002

Performance of the Generalized Minimum Residual (GMRES) Iterative Solution for the Magnetic Field Integral Equation

Sergey N. Makarov
Worcester Polytechnic Institute, makarov@wpi.edu

Ramanuja Vedantham

Performance of the generalized minimum residual (GMRES) iterative solution for the magnetic field integral equation

Sergey Makarov and Ramanuja Vedantham

Electrical and Computer Engineering Department, Worcester Polytechnic Institute, Worcester, Massachusetts, USA

Received 30 November 2000; revised 1 April 2002; accepted 2 May 2002; published 28 September 2002.

[1] The paper discusses a generalized minimum residual (GMRES) iterative solution of the magnetic field integral equation (MFIE) applied to frequency domain scattering problems at medium and high frequencies. First, the performance of the original MFIE is studied, for the perfectly electrically conducting (PEC) sphere. It is shown that the residual error and the solution error do not correlate with each other. Whereas the solution error has already reached a limiting value or even increases, the residual error continues to decrease very fast, typically exponentially. Second, the MFIE is combined with the normal projection of the primary integral equation for the surface magnetic field. Such a technique does not increase the computational complexity of the MFIE. At the same time, it gives a termination criterion for GMRES iterations since the residual error of the combined equation has a typical saturation behavior. In the saturation zone, the residual error and the solution error have approximately the same small value (a typical relative RMS error for the sphere is 1%). A very similar saturation behavior of the residual error has been observed for other tested PEC scatterers including a cube, a cylinder, and a sphere with one segment cut off (the so-called cat eye) at different frequencies. *INDEX TERMS:* 0644 Electromagnetics: Numerical methods; 0669 Electromagnetics: Scattering and diffraction; 0619 Electromagnetics: Electromagnetic theory; 0609 Electromagnetics: Antennas; *KEYWORDS:* MFIE, scattering, iterative solution, normal equation, inner resonances

Citation: Makarov, S., and R. Vedantham, Performance of the generalized minimum residual (GMRES) iterative solution for the magnetic field integral equation, *Radio Sci.*, *37*(5), 1072, doi:10.1029/2000RS002588, 2002.

1. Introduction

[2] The method of moments or the boundary integral equation method [*Peterson et al.*, 1998; *Poggio and Miller*, 1973] is one of the major computation tools for harmonic scattering and radiation from complex structures containing perfectly electrically conducting (PEC) bodies, such as antennas mounted on platforms, microstrip antennas and periodic two-and three-dimensional structures (metal optics). Iterative solutions of the magnetic field integral equation (MFIE) and/or electric field integral equation (EFIE) are currently receiving significant attention [*van der Berg*, 1991; *Kleinman and van der Berg*, 1991; *Hodges and Rahmat-Samii*, 1997; *Wang et al.*, 1999; *Sullivan and Carin*, 1999; *Rodrigues et al.*, 1997]. The main reason is the speed issue: they are fast and require $O(M^2)$ or fewer arithmetic operations to compute the surface current on a boundary divided into M boundary elements.

0048-6604/02/2000RS002588

[3] Generalized minimum residual (GMRES) method [*van der Vorst*, 2000; *Saad*, 2000] belongs to the so-called Krylov methods of the iterative solution. It is superior to the conjugate gradient method if more than a few iterations are employed [*van der Berg*, 1991; *Kleinman and van der Berg*, 1991]. Its idea is simple and powerful: retain all the previous iterations in memory and build the solution at the N-th iteration step as a linear combination of those vectors, with unknown coefficients. These coefficients are found from the minimum residual principle, which gives a system of linear equations of order $N + 1$ ("direct error minimization principle" [cf. *van der Berg*, 1991]). GMRES is the current de-facto non-symmetric system standard [*van der Vorst*, 2000]. The price for this ideal situation is that we have to store all the previous iterations; for many practical problems, however, GMRES takes a few tens of iterations to converge [*van der Vorst*, 2000]. Recent applications of GMRES solvers to various antenna problems underscore its excellent performance [*Yeng*, 1999; *Brown et al.*, 1999; *Botros, and Volakis*, 1999].

[4] An iterative solution can be controlled by tracking a residual error of the integral equation, at each iteration step [cf. *van der Berg*, 1991; *Kleinman and van der Berg*, 1991]. Unfortunately, the residual error is not an adequate measure of the solution error. For example, at the frequency of an internal resonance or at a close frequency, the residual error of MFIE/EFIE can be very small whereas the solution error remains high and even increases. The reason of such a behavior is well known and is connected with the development of parasitic resonant eigenmodes of the integral equation [*Peterson et al.*, 1998] when the number of iterations increases. At high frequencies the resonances are very common within any frequency band.

[5] A number of standard anti-resonant techniques exist such as the combined-field integral equation (CFIE), the combined source integral equation (CSIE), the method of inner points, and the dual-surface method [*Peterson et al.*, 1998]. In all these methods, the computational complexity becomes typically twice that of the original integral equation. Furthermore, we still cannot answer the question of how high is the solution error if the relative residual error reaches, for example, 5%.

[6] In this paper we test another mostly empirical technique, which is based on the augmented MFIE introduced by *Yaghjian* [1981]. This technique does not increase the computational complexity of the MFIE and, combined with the GMRES iterative method, leads to a few remarkable observations.

[7] In the case of a perfectly electrically conducting (PEC) sphere a ''saturation'' zone has been found after a fast convergence, where the solution error and residual error become approximately equal to each other. In the saturation zone, both the RMS errors are small (on the order of 1%) and change very little when the iteration number increases. The present observation holds at all tested frequencies including 6 lowest eigenfrequencies for the sphere.

[8] The presence of the saturation zone gives a straightforward termination rule for the iterative process. The iterations should be stopped if, for example, the difference between two subsequent residual errors becomes smaller than 1%. Such a stopping rule works well for the sphere and assures that the termination residual error will be approximately equal to the solution error. A very similar saturation zone has been observed for other tested structures including a cube, cylinder, cat eye, and rectangular metal meshes in a wide range of frequencies (the typical *ka* domain for scattering problems ranges from 1 to 30).

2. Theory

2.1. Integral Equation

[9] Below we denote by $\mathbf{x}$, $\mathbf{y}$ two arbitrary spatial points on a closed-body surface S; $\mathbf{n}$ is the unit normal at $\mathbf{x}$ or $\mathbf{y}$ pointing into the exterior of the surface S; $\mathbf{H}^i$, $\mathbf{H}^s$, $\mathbf{H}$ are incident, scattered, and the total magnetic field, respectively. The integral equation for the surface magnetic field on a surface of a PEC scatterer is considered in the form

$$\mathbf{H}(\mathbf{x}) = 2\int_S (\mathbf{n}\times\mathbf{H})\times\nabla_{\mathbf{y}} g(\mathbf{x},\mathbf{y})ds_y + 2\mathbf{H}^i(\mathbf{x}) \quad (1)$$

with the free-space Green's function $g(\mathbf{x},\mathbf{y}) = \exp(-jk|\mathbf{x}-\mathbf{y}|)/(4\pi|\mathbf{x}-\mathbf{y}|)$. Here, $k = \omega/c$ denotes the wave number, ω is the radian frequency, and c is the speed of light in the ambient medium. All time-varying quantities should obey time dependence $\exp(+j\omega t)$.

[10] Equation (1) is actually not the original MFIE but the MFIE augmented with the condition $\mathbf{n}\cdot\mathbf{H} = 0$ on the surface of a PEC scatterer and is originally due to [*Yaghjian*, 1981]. Vector multiplication of Equation (1) by the surface normal gives the standard MFIE, i.e.

$$\mathbf{J}_S(\mathbf{x}) = 2\mathbf{n}(\mathbf{x})\times\int_S \mathbf{J}_S(\mathbf{y})\times\nabla_{\mathbf{y}} g(\mathbf{x},\mathbf{y})ds_y + 2\mathbf{n}(\mathbf{x})\times\mathbf{H}^i(\mathbf{x}) \quad (2)$$

written in terms of the surface current, $\mathbf{J}_S = \mathbf{n}\times\mathbf{H}$. The scalar multiplication of Equation (1) by the surface normal gives the scalar equation

$$0 = 2\mathbf{n}(\mathbf{x})\cdot\int_S \mathbf{J}_S(\mathbf{y})\times\nabla_{\mathbf{y}} g(\mathbf{x},\mathbf{y})ds_y + 2\mathbf{n}(\mathbf{x})\cdot\mathbf{H}^i(\mathbf{x}) \quad (3)$$

since $\mathbf{n}\cdot\mathbf{H} = 0$ is enforced on the surface of a PEC scatterer. Equations (2) and (3) both follow from Equation (1) and from the boundary condition $\mathbf{n}\cdot\mathbf{H} = 0$. However, Equation (3) cannot be derived from the tangential-field MFIE directly and is in that sense formally independent. To simplify further notations we rewrite Equations (2) and (3) in the operator form, i.e.

$$R\mathbf{J}_S = \mathbf{J}_S(\mathbf{x}) - 2\mathbf{n}(\mathbf{x})\times\int_S \mathbf{J}_S(\mathbf{y})\times\nabla_{\mathbf{y}} g(\mathbf{x},\mathbf{y})ds_y, \qquad R\mathbf{J}_S = 2\mathbf{n}(\mathbf{x})\times\mathbf{H}^i(\mathbf{x}) \quad (4)$$

$$Q\mathbf{J}_S = -2\mathbf{n}(\mathbf{x})\cdot\int_S \mathbf{J}_s(\mathbf{y})\times\nabla_{\mathbf{y}} g(\mathbf{x},\mathbf{y})ds_y, \qquad Q\mathbf{J}_S = 2\mathbf{n}(\mathbf{x})\cdot\mathbf{H}^i(\mathbf{x}) \quad (5)$$

Below, we will be testing a combination of Equations (2) and (3). It is expected that such a combination will eliminate the spurious resonances similar to the primary Yaghjian's model [*Yaghjian*, 1981]. It also has some other practical advantages as discussed in the following text.

2.2. Iterative Solution

[11] The following formulation of GMRES is applied to the MFIE equation [cf. also *van der Berg*, 1991, pp. 30–32]. Subsequent iterations $\mathbf{J}^0$, $\mathbf{J}^1$, $\mathbf{J}^2$, ... necessary to maintain an approximate solution of Equation (2) (spanning vectors of the corresponding Krylov subspace) are found in the form

$$\mathbf{J}^N = \mathbf{r}^{N-1} \, at \, N \geq 1; \tag{6}$$

where $\mathbf{r}^{N-1}$ is the residual of the integral equation calculated after substitution of an approximate solution obtained at the previous iteration step. Each residual is orthogonalized with respect to the surface normal:

$$\mathbf{r}^N(\mathbf{x}) \rightarrow \mathbf{r}^N(\mathbf{x}) - \mathbf{n}(\mathbf{x})\big(\mathbf{r}^N \cdot \mathbf{n}(\mathbf{x})\big) \tag{7}$$

[12] The starting guess, $\mathbf{J}^0$, at plane wave incidence may be found from the physical optics (PO) approximation [cf. *Poggio and Miller*, 1973],

$$\mathbf{J}^0(\mathbf{x}) = \begin{cases} 2\mathbf{n}(\mathbf{x}) \times \mathbf{H}^i(\mathbf{x}) & \text{illuminated domain} \\ 0 & \text{shadow domain.} \end{cases} \tag{8}$$

One of the shortcomings of the PO approximation is the abrupt discontinuity near the terminator, which can be a potential source of developing oscillations close to the resonant frequencies. At plane wave incidence, the plane wave approximation (PWA)

$$\mathbf{J}^0(\mathbf{x}) = (1 - \cos(\mathbf{k}, \mathbf{n}(\mathbf{x})))\big(\mathbf{n}(\mathbf{x}) \times \mathbf{H}^i(\mathbf{x})\big) \tag{9}$$

is a considerably better starting point than PO. Here, $\mathbf{k}$ is the wave vector of the incident plane wave.

[13] The solution for the surface current at the N-th iteration step is sought in the form $\mathbf{J}_S^N = a_0\mathbf{J}^0 + a_1\mathbf{J}^1 + \ldots + a_N\mathbf{J}^N$, where $a_0, a_1, \ldots, a_N$ are unknown (complex) coefficients. The minimum residual variation yields a system of linear equations for those coefficients of order $N+1$. We solve this system directly [*van der Berg*, 1991] instead of the orthogonalization of the basis vectors $\mathbf{J}^0$, $\mathbf{J}^1$, $\mathbf{J}^2$, ... etc. [*Saad*, 2000]. No preconditioner is used in the present iterative solution [cf., e.g., *Adams and Brown*, 1999].

2.3. Control of Convergence

[14] The measure of convergence is the RMS relative residual error, E_N^R,

$$E_N^R = \frac{\|R\mathbf{J}_S^N\|}{\|2\mathbf{n} \times \mathbf{H}^i\|}, \|\mathbf{J}\| := \left(\int_S |\mathbf{J} \cdot \mathbf{J}| \, ds_y \right)^{1/2} \text{on S} \tag{10}$$

of the magnetic field integral equation (2). Another quantity of interest is the RMS residual error of integral equation (3), i.e.

$$E_N^Q = \frac{\|Q\mathbf{J}_S^N\|}{\|2\mathbf{n} \times \mathbf{H}^i\|}, \|\mathbf{J}\| := \left(\int_S |\mathbf{J} \cdot \mathbf{J}| \, ds_y \right)^{1/2} \text{on S} \tag{11}$$

The RMS solution error E_N^A with respect to the exact analytical solution for the surface current $\mathbf{J}_s^A$ on the surface of a PEC sphere [*Sengupta*, 1987; *Born and Wolf*, 1998] is also introduced, i.e.

$$E_N^A = \frac{\|\mathbf{J}_S^N - \mathbf{J}_S^A\|}{\|\mathbf{J}_S^A\|} \text{on} \, S \tag{12}$$

The Mie series for the sphere surface current is given by *Sengupta* [1987].

[15] All three errors (10)–(12) are calculated at every iteration step N and provide a measure of accuracy of the iterative solution. We must emphasize the principal difference between the solution error and the residual error. The solution error will always be nonzero for a finite number of unknowns. The primary source of the solution error is a piecewise constant representation of the current. Another source of the solution error is the inaccuracy of the iterative solution itself, due to insufficient number of iterations. One more and sometimes critical source of the solution error is the development of parasitic eigenmodes. The residual error norm, however, can be made arbitrarily small in the absence of roundoff error for any number of unknowns. Although both errors clearly have different nature, in practice, the residual error is widely used as a measure of the solution errors. It will be shown later that, under certain conditions, both errors may strongly correlate as long as the solution error is still above the discretization limit.

3. PEC Sphere at Resonant and Nonresonant Frequencies

3.1. Performance of the Pure MFIE

[16] In this section a comparison of the numerical solution for the sphere with the analytical solution is presented. The comparison is given in terms of the surface current RMS error. It has long been known that large local errors in surface currents may be observed in spite of excellent agreement in the far-field [*Peterson et al.*, 1998]. However, a small surface current error guarantees us the smallness of the far-field error. Following *Sengupta* [1987] we assume a plane wave incident upon the sphere of radius a in the direction of the negative z-axis and polarized along the y-axis, i.e.

$$\mathbf{H}^i = (0 \;\; -Y \;\; 0)\exp(-jkz) \tag{13}$$

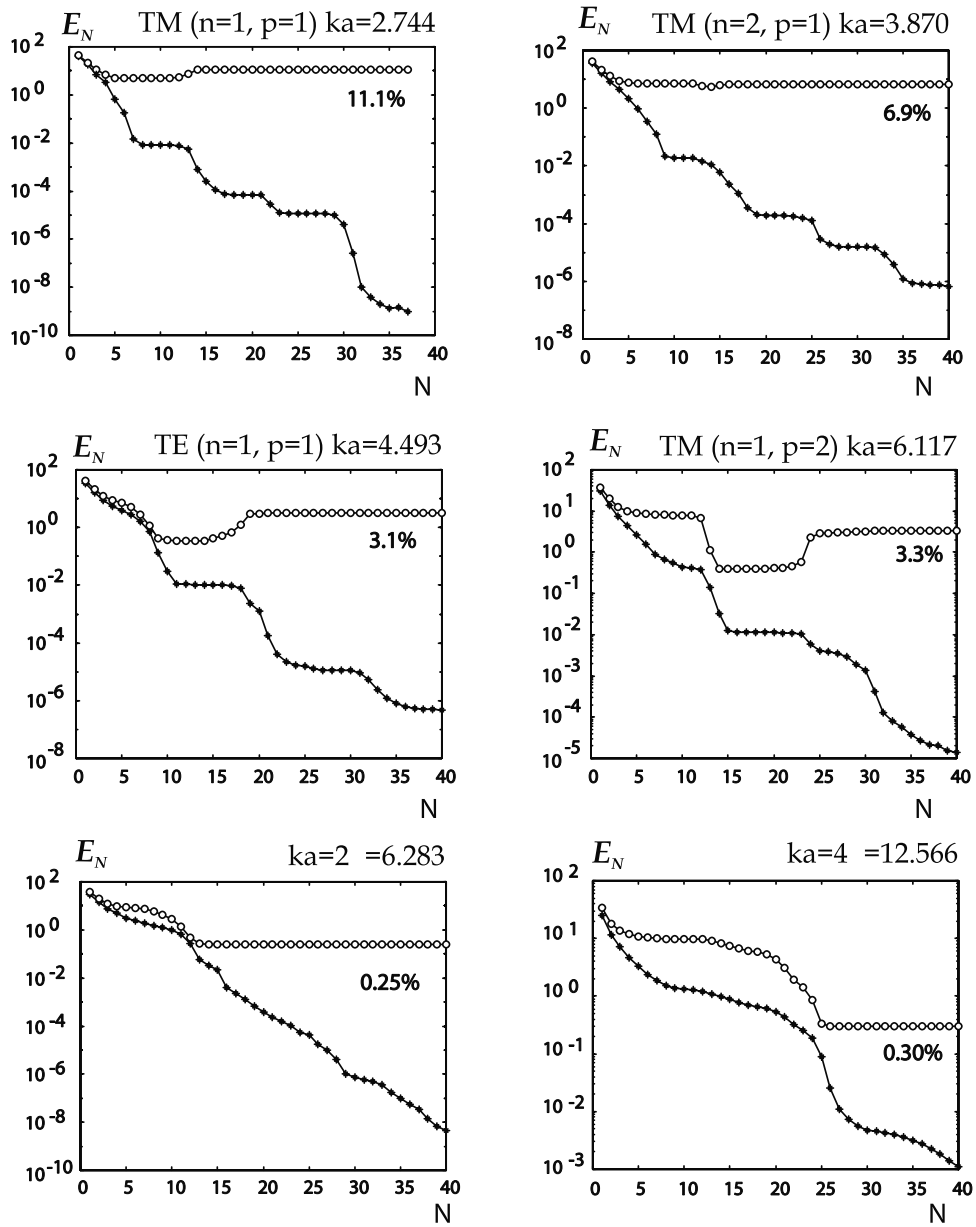

Figure 1. Residual, E_N^R, and solution, E_N^A, RMS errors (%) for the PEC sphere as functions of the iteration number, N, at different frequencies (MFIE). Stars, residual error; circles, solution error. The solution error at the 40th iteration is given on the body of the graph for each computed ka value.

A sphere surface (of radius a = 1 m) is modeled by 6,096 plane triangular and rectangular patches of nearly the same size. The surface current is constant across each boundary element. Figure 1 shows the error curves for pure MFIE at six different ka values including four lowest resonances of TM (ka = 2.744, 3.870, 6.117) and TE (ka = 4.493) types [*Balanis*, 1989]. The residual error E_N^R is denoted by stars, whereas the solution error E_N^A is denoted by circles. Both errors are the functions of the iteration number N.

[17] A few observations can be made from Figure 1. First, the GMRES performs quite well at non-resonant frequencies. In the case of $ka = 2\pi$ and $ka = 4\pi$, a relatively small error with respect to the exact solution is

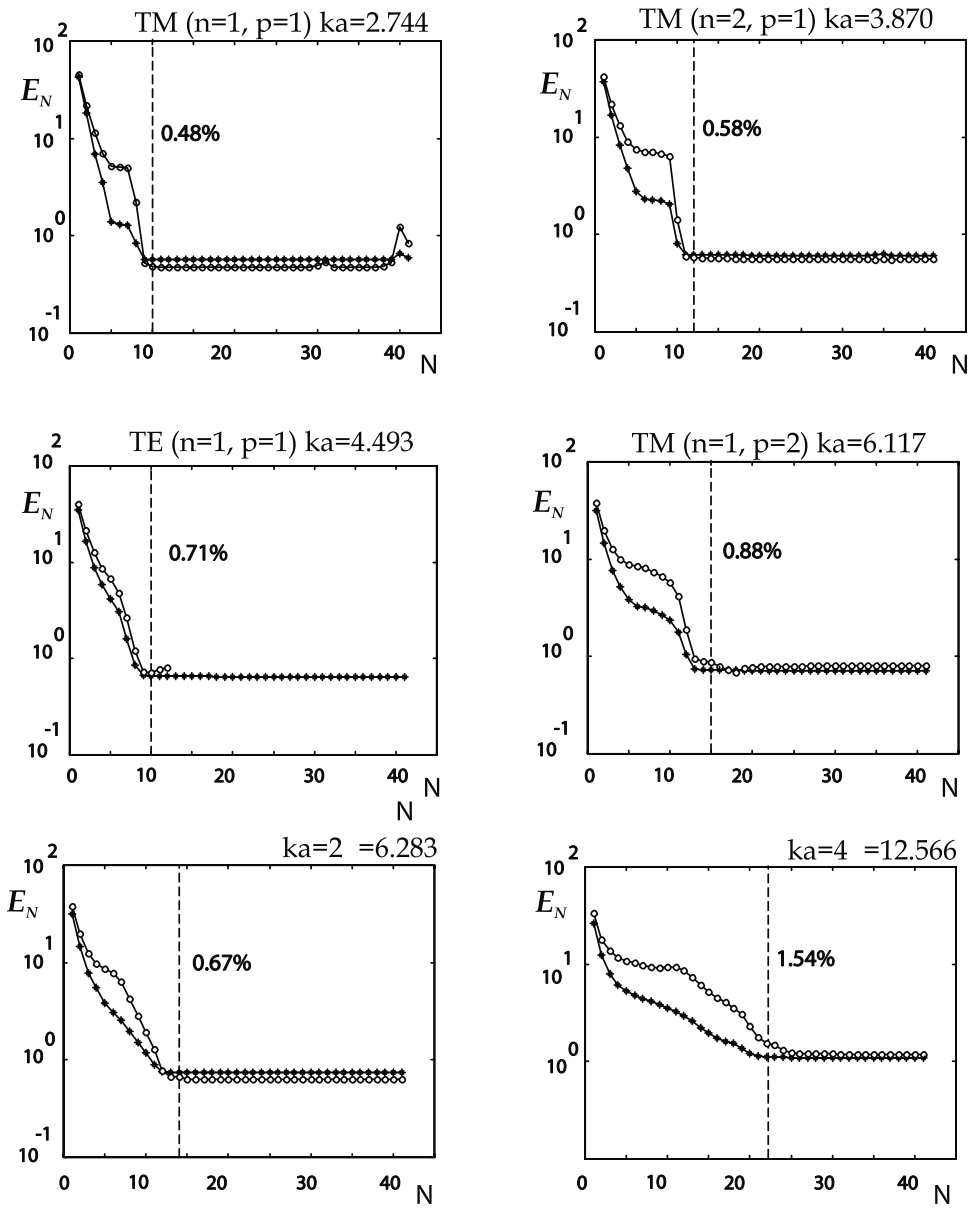

Figure 2. Residual, E_N^R, and solution, E_N^A, RMS errors (%) for the PEC sphere as functions of the iteration number, N, at different frequencies (modified MFIE with $\alpha = 0.25$). Stars, residual error; circles, solution error. Dashed lines indicate the termination number, N_R, obtained from the 1%-variation rule. The solution error at the termination is given on the body of the graph for each computed *ka* value.

achieved, on the order of 0.3%, after 15th and 25th iteration, respectively. At the exact resonant frequencies (*ka* = 2.744, 3.870, 4.493, and 6.117), however, the residual error decreases by several orders of magnitude whereas the solution error remains high and even increases when iterations progress. Typical limiting values of the solution error range from 3 to 11%. (If a direct solver is employed, the resonant behavior of MFIE is very sensitive to the particular frequency value chosen close to the resonant frequency. For an iterative solution, the sensitivity is much lower: the solution error has a typical Gaussian shape centered at the resonant frequency. Therefore, we restrict ourselves to four significant digits for the resonant frequency.)

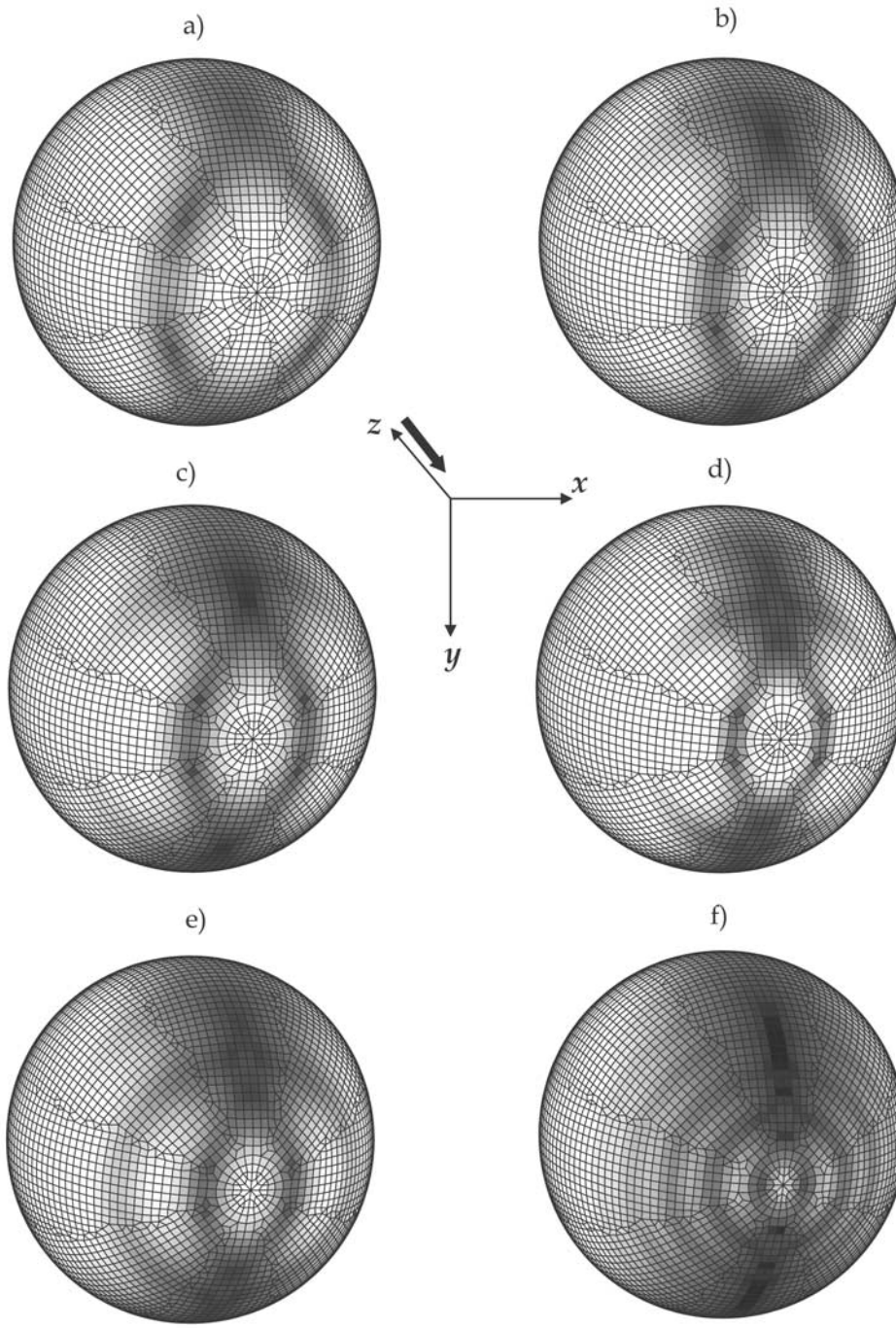

Figure 3. Magnitude of the surface current, $\mathbf{J}_s$, in the shadow zone of the sphere. (a) $ka = 2.744$, (b) $ka = 3.870$, (c) $ka = 4.493$, (d) $ka = 6.117$, (e) $ka = 2\pi$, (f) $ka = 4\pi$. Grey scale extends from 0 (black) to 0.7 and above (white). The incident plane wave has the amplitude 1. The current magnitude over the entire sphere surface changes from approximately 2 (top of the illuminated zone) to 0 (certain regions in the shadow area).

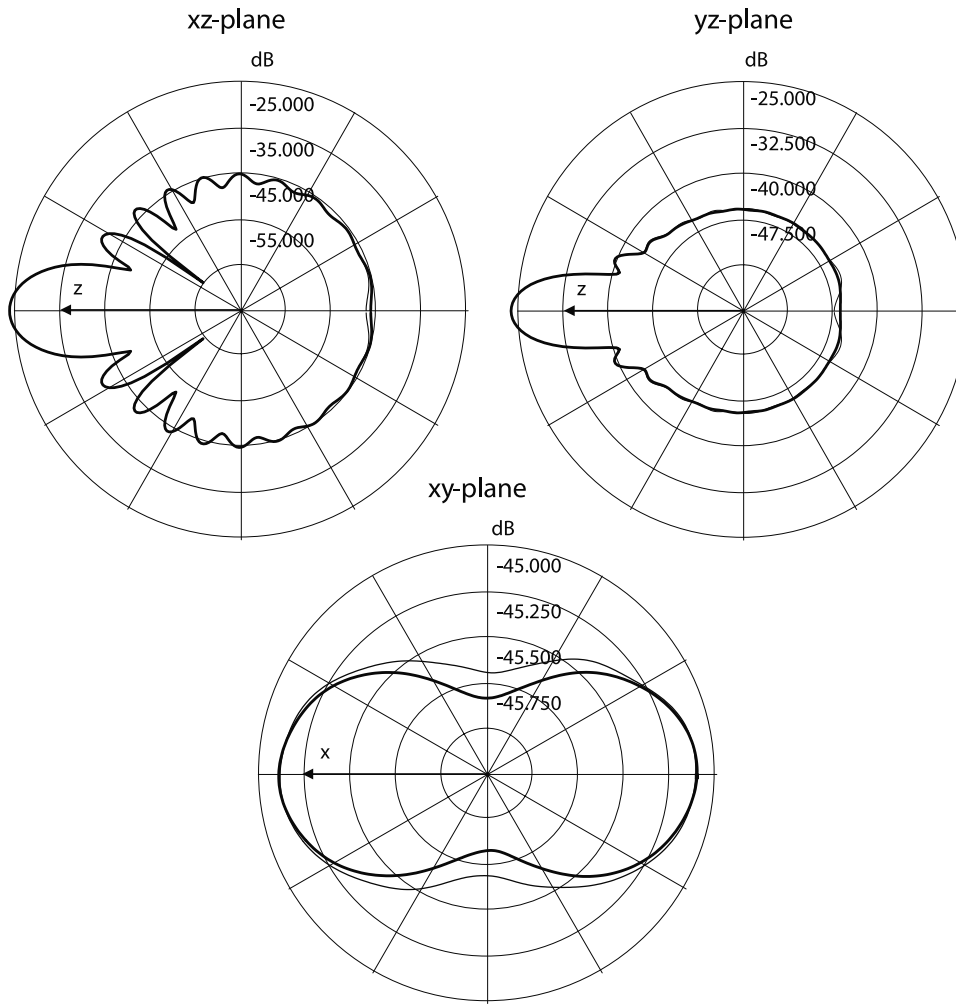

Figure 4. Directivity patterns for the sphere with 6,096 elements at $ka = 4\pi$. The solution based on the exact surface current is given by a thick line. The thin line shows the result of the termination iteration ($N_R = 22$).

[18] In both cases (at resonant and non-resonant frequencies) there seems to be no correlation between the residual error and the solution error. When the solution error has already reached a limiting value (due to discretization accuracy or parasitic eigenmodes, or other reasons), the residual error continues to decrease very fast, typically exponentially. Note that for structures different from the sphere, only the residual error is available. Therefore we cannot estimate the solution error for those structures based on the data for the residual error.

3.2. Performance of a Modified MFIE

[19] A way is further discussed of how to correlate the residual and the solution error. We have added Equation (3) multiplied by $j\alpha\mathbf{n}$ to the magnetic field integral equation. Typically, $\alpha = 0.1-0.5$. Such an addition does not require any additional computational complexity since either the normal or the tangential projection of the surface integral

$$\int_S \mathbf{J}_S(\mathbf{y}) \times \nabla_y g(\mathbf{x}, \mathbf{y}) ds_y \qquad (14)$$

are employed. Figure 2 shows the error curves for the modified MFIE at $\alpha = 0.25$. The same ka values are considered corresponding to those in Figure 1. The residual error E_N^R is again denoted by stars, and the solution error E_N^A is denoted by circles.

[20] Compared to Figure 1, a completely different behavior of the residual error is observed in Figure 2.

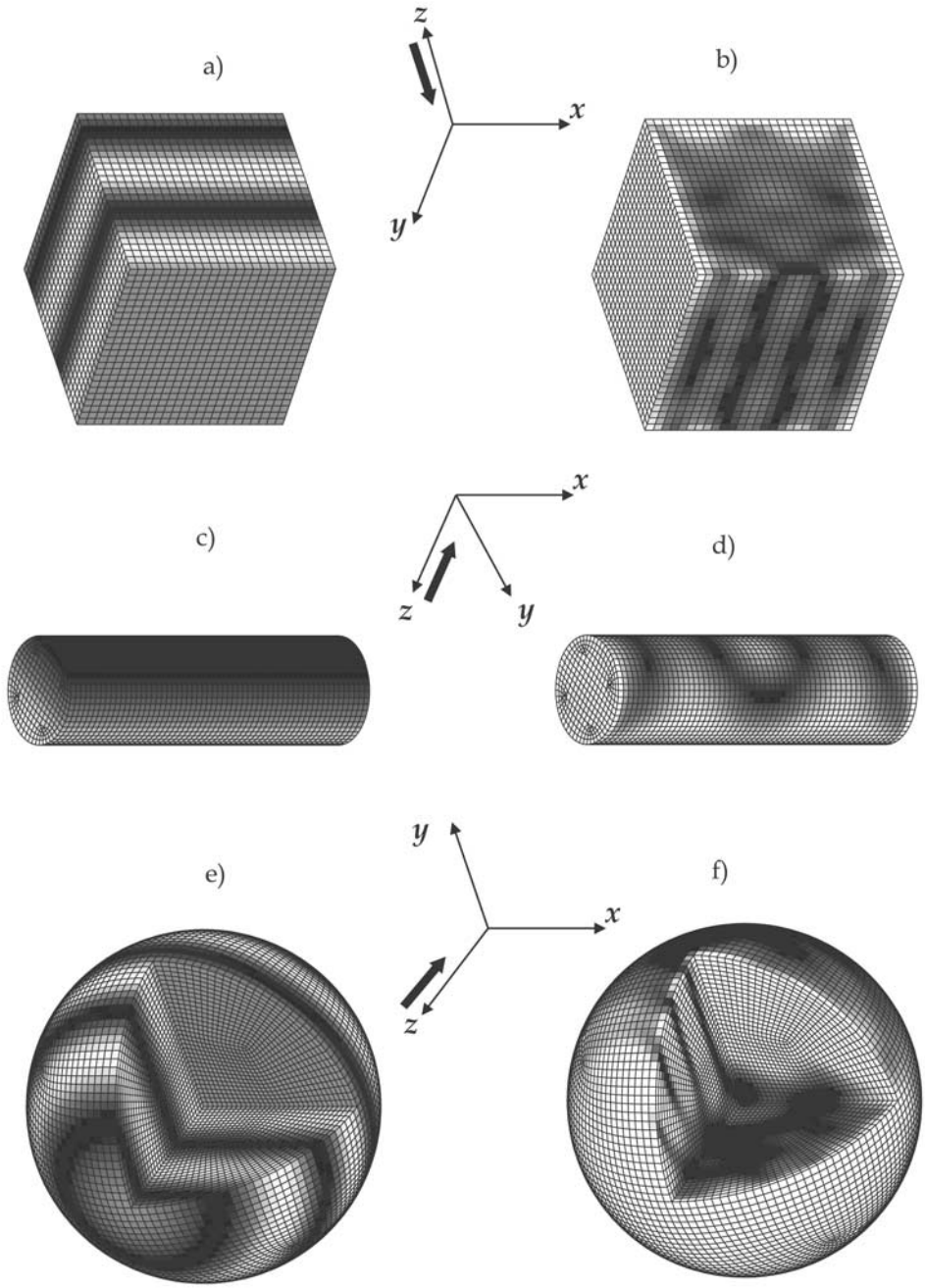

Figure 5. Phase of the incident field (left) and the magnitude of the total surface current $\mathbf{J}_s$ (right) for three scatterers: a cube with the side $a = 1$ m, a 1:4 cylinder of the length $a = 1$ m, and a cat eye of the radius $a = 1$ m, all at $ka = 4\pi$. The incident plane wave has amplitude 1. For the surface current magnitude, grey scale extends from 0.2 (black) to 0.7 (white) for the cube, from 0.2 to 1.2 for the cylinder, and from 0.5 to 1.5 for the cat eye.

Table 1. Initial Residual Error E_1^R, Termination Number N_R, and the Termination Residual Error $E_{N_R}^R$ for the PEC Cube at Different *ka* and $\alpha = 0.25$[a]

ka	E_1^R, %	N_R	$E_{N_R}^R$, %
2.744	48.0	9	5.0
3.870	46.8	10	4.0
4.493	45.2	13	3.7
6.117	39.0	14	3.3
2π	38.4	16	3.3
4π	29.4	21	2.8

[a] The side, *a*, of the cube is equal to 1 m.

Table 3. Initial Residual Error E_1^R, Termination Number N_R, and the Termination Residual Error $E_{N_R}^R$ for the PEC Cat Eye Structure at Different *ka* and $\alpha = 0.5$[a]

ka	E_1^R, %	N_R	$E_{N_R}^R$, %
2.744	50.2	16	5.5
3.870	50.8	21	5.2
4.493	49.6	20	6.3
6.117	46.3	17	9.7
2π	46.1	13	9.7
4π	39.0	29	9.3

[a] The radius of the corresponding sphere, *a*, is equal to 1 m.

After a relatively fast initial drop, the residual error tends to an asymptotically stable value, which approximates the solution error. A dashed line in Figure 2 indicates an iteration number, N_R, where the relative change in the residual error per iteration becomes smaller than 1%. We will use that number as a termination criterion of the GMRES iteration process. The solution error corresponding to the number N_R is shown on the body of the graph. It varies from 0.48% ($ka = 2.744$) to 1.54% ($ka = 4\pi = 12.566$) and generally increases with increasing frequency. It can be observed that the 1%-rule gives us a convenient termination criterion for all the six cases depicted in Figure 2. The corresponding termination error with respect to the exact solution is typically smaller than or equal 1%. Analogous observations can be made at higher frequencies up to $ka = 8\pi = 25.133$ including higher resonances. Similar results also hold at $0.1 < \alpha < 0.5$.

[21] The case of the TE mode ($ka = 4.493$) is the worst one. The solution error tends to increase after reaching a "lowest" point. However, even in that case, the termination criterion cuts the meaningless rest of iterations and gives us the termination error with respect to the exact solution of 0.71% at $N = 10$. This seems to be a very satisfactory result for the essentially stand-alone MFIE.

Table 2. Initial Residual Error E_1^R, Termination Number N_R, and the Termination Residual Error $E_{N_R}^R$ for the PEC 1:4 Cylinder at Different *ka* and $\alpha = 0.5$[a]

ka	E_1^R, %	N_R	$E_{N_R}^R$, %
2.744	48.5	10	3.9
3.870	49.0	10	4.2
4.493	49.8	10	4.3
6.117	51.9	8	4.5
2π	52.1	8	4.4
4π	53.5	11	4.4

[a] The length, *a*, of the cylinder is equal to 1 m.

[22] Figure 3 shows the magnitude distribution of the surface current in the shadow zone of the sphere at the termination. The termination numbers are taken from Figure 2. The same *ka* values are considered, in the same sequence. To elucidate the shadow zone topography, grey scale extends from 0 (black) to 0.7 (white). All magnitudes greater than 0.7 are marked white. The incident plane wave (along the negative *z*-direction; *y*-polarized) is of amplitude 1. The current magnitude over the entire sphere surface changes from approximately 2 (top of the illuminated zone) to 0 (certain regions in the shadow area).

[23] If the RMS error in the surface currents is smaller than 1%, the differences in the far-field are hardly seen. As an example, Figure 4 shows the directivity patterns for the sphere corresponding to the case of $ka = 4\pi = 12.566$, where the solution error of 1.54% at the termination, $N_R = 22$, has the largest possible value. Thick line is the exact solution (obtained using the exact surface current distribution on the sphere surface) whereas thin line is the result of the termination iteration at $N_R = 22$. The agreement is generally good except for small oscillations at forward scattering.

4. Arbitrary PEC Scatterers

4.1. Termination Criterion

[24] The model of a modified MFIE introduced in the last section is tested here for other PEC scatterers, including a cube with 3,750 boundary elements, a 1:4 cylinder with 3,620 boundary elements, and a cat eye structure with 7,911 boundary elements (compare Figure 5 below in the text) at plane wave incidence. The side of the cube, the cylinder length, and the cat eye radius are all denoted by *a*, and are all equal to 1 m. The incident field is the same as in section 3.1.

[25] It has been found that the behavior of the residual error is very similar to that from section 3.2 and Figure 2 related to the sphere. The asymptotically stable saturation zone appears for these structures, typically after the

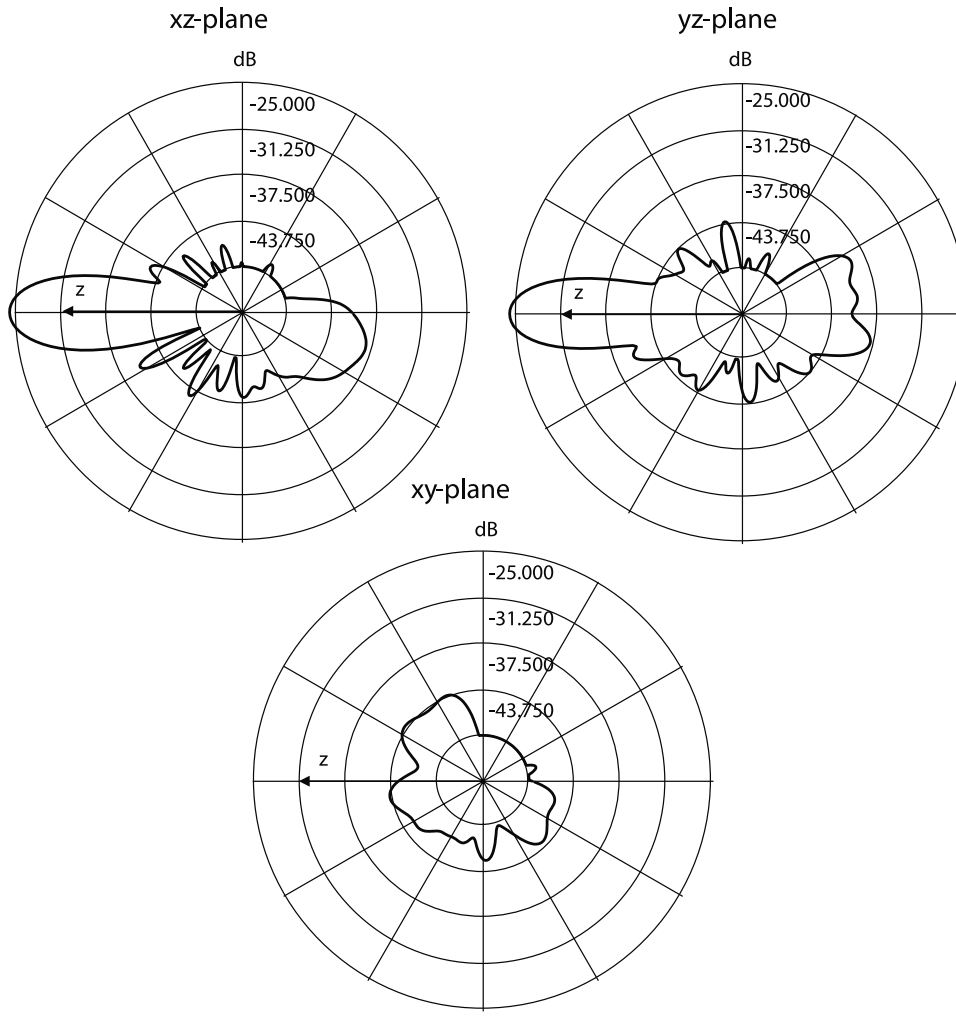

Figure 6. Directivity patterns for the cat eye with 7,911 elements at $ka = 4\pi$. The curve shows the result of the termination iteration ($N_R = 29$).

10th–20th iteration. In that zone, the 1%-variation criterion can be applied to the residual error to terminate the iterations. By analogy with the sphere, the termination solution error should be expected to be on the same order of magnitude. To be consistent with the sphere solution, we consider the same *ka* values as above.

[26] Tables 1–3 give the starting residual error, the termination residual error, and the termination iteration number for the cube, cylinder, and the cat eye at different *ka*. The results are in line with the observation for the sphere. However, the termination error typically becomes larger. This is especially true for the cat eye structure at high frequencies, where the termination error could reach 9.3% at $ka = 4\pi = 12.566$. This structure is characterized by the multiple reflections within the cat eye and a higher number of boundary elements are necessary to improve the method performance. Figure 5 shows the phase of the incident wave (left) and the surface current magnitude distribution (right) for the three structures under study at $ka = 4\pi = 12.566$. The termination iteration number was obtained from Tables 1–3. The plane wave incidence (along the negative *z*-axis) is shown by the arrows. The polarization of the incident wave is always in the *y*-direction. To underscore the topography of the surface currents, different scales are employed for the surface currents. Figure 6 gives the directivity patterns for the cat eye at $ka = 4\pi = 12.566$.

4.2. Effect of the Number of Boundary Elements

[27] Together with the cube divided into 3,750 square patches, a cube of the same size but with 9,600 square

Table 4. Initial Residual Error E_1^R, Termination Number N_R, and the Termination Residual Error $E_{N_R}^R$ for the PEC Cube at Different *ka* and $\alpha = 0.25$[a]

ka	E_1^R, %	N_R	$E_{N_R}^R$, %
2.744	48.2	9	4.5
3.870	46.9	10	3.7
4.493	45.3	13	3.4
6.117	39.2	14	3.0
2π	38.6	16	3.0
4π	29.6	21	2.5

[a] The side, *a*, of the cube is equal to 1 m, with 9600 boundary elements.

boundary elements is considered. Table 4 indicates the corresponding solution performance, including the termination error and the termination number. Compared to the results for the first cube (Table 1) the termination number remains exactly the same. The termination error becomes somewhat smaller. However, the improvement is not as high compared to the computer efforts needed to complete the solution (the processor time is 6 times higher for the second cube).

[28] This result is generally in line with the requirement of at least 6 boundary elements per wavelength, which is eventually satisfied for each cube, in the frequency range under test. Therefore, the further increase of the discretization accuracy has a little effect on the solution performance.

5. Summary and Conclusions

[29] A method is proposed and tested for the GMRES solution of the magnetic field integral equation, involving the problem of internal resonances. The specific numerical examples given are for PEC structures. The MFIE is modified by adding the normal projection of the augmented Yaghjian's integral equation for the *H*-field on the scatterer surface [*Yaghjian*, 1981]. In contrast to CFIE and CSIE, the present approach is not expected to completely eliminate the singularities present in the MFIE (the homogeneous solutions of MFIE) and the associated problems. However, it might have a few practical advantages: (1) No additional computational complexity is involved with respect to the pure MFIE (the amount of computations slightly increases). (2) The method gives a natural termination criterion for the iteration process, based on the typical ''saturation'' behavior of the residual error. (3) At the termination, the solution error and the residual error have the same order of magnitude, at least for the PEC sphere.

[30] The test for the PEC sphere shows the high accuracy of the present method, including both nonresonant and resonant frequencies (TM and TE modes).

[31] Open questions are further understanding of the underlying mathematics behind the residual error behavior and the behavior of the solution error. The accuracy of the present approach is not completely satisfactory and could perhaps be improved, especially for non-convex scatterers and at the resonant conditions.

[32] **Acknowledgments.** The authors are thankful to three anonymous referees for valuable comments. This work is supported by National Science Foundation grant ECS-0096395.

References

Adams, R. J., and G. S. Brown, Stabilization procedure for electric field integral equation, *Electron. Lett.*, *35*, 2015–2016, 1999.

Balanis, C. A., *Advanced Engineering Electromagnetics*, John Wiley, New York, 1989.

Born, M., and E. Wolf, *Principles of Optics*, 6th ed., chap. 13, Cambridge Univ. Press, New York, 1998.

Botros, Y. Y., and J. L. Volakis, Preconditioned generalized minimum residual iterative scheme for perfectly matched layer terminated applications, *IEEE Microwave Guided Wave Lett.*, *9*, 45–47, 1999.

Brown, A. D., J. L. Volakis, L. C. Kempel, and Y. Y. Botros, Patch antennas on ferromagnetic substrates, *IEEE Trans. Antennas Propag.*, *47*, 26–32, 1999.

Hodges, R. E., and Y. Rahmat-Samii, An iterative current-based hybrid method for complex structures, *IEEE Trans. Antennas Propag.*, *45*, 265–276, 1997.

Kleinman, R. E., and P. M. van der Berg, Iterative methods for solving integral equations, in *Application of Conjugate Gradient Method to Electromagnetics and Signal Analysis, Prog. Electromagn. Res.*, vol. 5, edited by T. K. Sarkar, chap. 3, pp. 67–102, Elsevier Sci., New York, 1991.

Peterson, F., S. L. Ray, and R. Mittra, *Computational Methods for Electromagnetics*, IEEE Press, Piscataway, N.J., 1998.

Poggio, J., and E. K. Miller, Integral equation solutions of three-dimensional scattering problems, in *Computer Techniques for Electromagnetics*, 2nd ed., edited by R. Mittra, pp. 169–264, Pergamon, Tarrytown, N.J., 1973.

Rodrigues, J. L., F. Obelleiro, and A. G. Pino, Iterative solutions of MFIE for computing electromagnetic scattering of large open-ended cavities, *IEE Proc. Part H, Microwaves Antennas Propag.*, *144*, 141–144, 1997.

Saad, Y., *Iterative Methods for Sparse Linear Systems*, 2nd ed., PWS, Boston, Mass., 2000.

Sengupta, D. L., The sphere, in *Electromagnetic and Acoustic Scattering by Simple Shapes*, 2nd ed., edited by J. J. Bowman, T. B. A. Senior, and P. L. E. Uslenghi, pp. 2353–2415, Taylor and Francis, Philadelphia, Pa., 1987.

Sullivan, A., and L. Carin, Scattering from complex bodies using a combined direct and iterative technique, *IEEE Trans. Antennas Propag.*, *47*, 33–39, 1999.

van der Berg, P. M., Iterative schemes based on minimization of a uniform error criterion, in *Application of Conjugate Gra-*

dient Method to Electromagnetics and Signal Analysis, Prog. Electromagn. Res., vol. 5, edited by T. K. Sarkar, chap. 2, pp. 27–65, Elsevier Sci., New York, 1991.

van der Vorst, H. A., Krylov subspace iterations, *Comput. Sci. Eng.*, *2*, 32–37, 2000.

Wang, C.-F., F. Ling, J. Song, and J.-M. Jin, A fast algorithm for solving CFIE of EM scattering, paper presented at 1999 IEEE International Symposium, Antennas and Propag. Soc., Orlando, Fla., 1999.

Yaghjian, A. D., Augmented electric-and magnetic-field integral equations, *Radio Sci.*, *16*, 987–1001, 1981.

Yeng, M. S., Single integral equation for electromagnetic scattering by three-dimensional homogeneous dielectric objects, *IEEE Trans. Antennas Propag.*, *47*, 1615–1622, 1999.

S. Makarov and R. Vedantham, Electrical and Computer Engineering Department, Worcester Polytechnic Institute, 100 Institute Road, Worcester, MA 01609-2280, USA. (makarov@wpi.edu)